*Mol. Cryst. Liq. Cryst.*, Vol. 543: pp. 177/[943]–186/[952], 2011

ISSN: 1542-1406 print/1563-5287 online
DOI: 10.1080/15421406.2011.569521

Taylor & Francis
Taylor & Francis Group

# Nonlinear Electromagnetic Waves in a Nematic Slab

CARLOS I. MENDOZA[1] AND J. ADRIAN REYES*[2]

[1]Instituto de Investigaciones en Materiales, Universidad Nacional Autónoma de México, México D. F., Mexico
[2]Universidad Autónoma Metropolitana, Ixtapalapa, México D. F., Mexico



*We consider a nonlinear system formed by a thin nematic slab immersed in vacuum, submitted to the action of a high-intensity normally-incident plane electromagnetic wave. We solve simultaneously, by using a numerical scheme, the director's orientational configuration and Maxwell's equations for this system using homeotropic soft boundary conditions. For a given field intensity, we find multiple equilibrium director's configurations. In addition, we study the reflectance versus the wavelength and the field intensity.*

**Keywords** Elastic properties; electro-optic effects; nematic molecules; nonlinear optics

## 1. Introduction

The giant optical nonlinear response-a factor of 6–10 orders of magnitude larger [1,2] than that of doped glasses – makes feasible to consider the deformation provoked in the nematic fiber by the same electromagnetic field which is propagated. Several systems for which a nematic is submitted to a large intensity optical field whose configuration is not anchored to waveguide boundary conditions, give rise to spatial patterns and solitons [3–5]. The basic mechanism which governs these time independent patterns is the balance between the nonlinear refraction (self-focussing) and the spatial diffraction of the nematic. A study of these experiments using separation of scales [6,7] shows that the field amplitude at the center of a gaussian beam (inner solution), follows a nonlocal non linear Schroedinger equation which is able to describe the undulation and filamentation observed in the experiments.

Laser beam propagation in azobenzene liquid crystals in waveguiding configuration has been considered in [8]. They found that spatial solitons can be formed at microwatt power levels of a He-Ne laser beam and they analyzed several well-known processes of nonlinear propagation such as undulation of solitons, their interaction

*On leave from Instituto de Fisica UNAM.
Address correspondence to J. Adrian Reyes, Universidad Autónoma Metropolitana, Ixtapalapa, Apdo Postal 55534 09340, México D. F., Mexico. Tel.: 52-55-56225178; E-mail: adrian@fisica.unam.mx

and merging. *Cis-trans* isomerization of azobenzene molecules and related change in the LC order parameter is the underlying mechanism of optical nonlinearity that makes possible formation of solitons. In [9], it is shown that optical reorientation nonlinearity in twisted nematic liquid crystalline waveguides is large enough to observe spatial solitons with milliwatts of light power.

It is important to stress that in general nematicons [7] and other spatial solitons found in nonlinear systems are coherent structures formed in regions of the system where both orientational and optical fields have lost influence from the boundary conditions. In this sense, all these balanced and robust profiles of energy, called solitons, are asymptotic solutions which are not to be forced by strict boundary conditions but they have to satisfy only certain mean-field matching conditions. Indeed, as long as the confining cell of the liquid crystal turns to be larger, the bias-free confinement is more notorious [10]. In this manuscript we are interested instead in analyze the role played by the boundary conditions within the optical-orientational non linear coupling of a nematic slab.

There are some pioneering studies in the literature [11–13] where nonlinear electromagnetic modes in nematic liquid crystal confined under different geometries are considered. For a slab waveguide [11] and starting from Maxwell's equations and from the torque equation for the nematic director, it was derived a set of nonlinear differential equations and it was exactly solved by a numerical technique based on the continuation method for the case of planar initial alignment of the nematic director. The director reorientation induced by the guided light itself gives rise to such strong nonlinear effects as self-confinement and intrinsic optical bistability. In our work, we instead solve simultaneously the orientational and electromagnetic boundary value problems parameterized by the optical field intensity.

Most of the optical calculations in nematic systems have been done by assuming hard anchoring boundary conditions for the nematic director. This is inconsistent with the high intensity of the electromagnetic field since in the plates the electric force can be stronger than the surface elastic force as has been shown before [14]. Moreover, when liquid crystals are confined to small cavities, its effect is found to be significant, particularly when elastic energies imposed by the confining volume compete with molecular anchoring energies [15]. Hence we cannot ignore surface elastic terms compared with both bulk elastic terms and electric bulk contributions.

The purpose of the present paper is to analyze the nonlinear effects produced by a high intensity plane wave impinging the nematic homeotropic slab by assuming soft anchoring boundary conditions. The outline of the paper is as follows: in Sec. 2, we find the nematic configurations assuming arbitrary anchoring conditions, in Sec. 3, we consider the case of transverse magnetic field, in Sec. 4 we present the results of the calculation, and finally, in Sec. 4, we discuss and summarize our results.

## 2. Nematic Configuration

Let us consider a nematic slab with homeotropic boundary conditions as depicted in Figure 1. This means that the easy direction for the molecular orientation is the direction perpendicular to the plates. However, due to the softness of the anchoring at the boundaries, the nematic is not necessarily perpendicular to the plates.

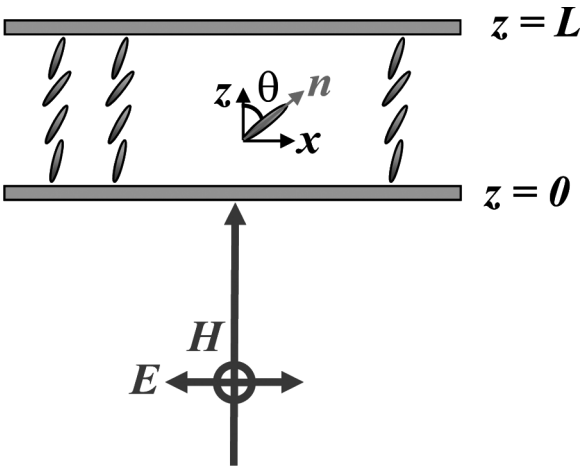


**Figure 1.** Schematics of a nematic slab subjected to a normally incidence plane wave.

The continuous medium description of the nematic is governed by the elastic free energy, $F$ [16], given by

$$F_{el} = \frac{1}{2}\int_V [K_1(\nabla\cdot\hat{n})^2 + K_2(\hat{n}\cdot\nabla\times\hat{n})^2 + K_3(\hat{n}\times\nabla\times\hat{n})^2 - K_{24}\nabla\cdot[\hat{n}\nabla\cdot\hat{n} + \hat{n}\times\nabla\times\hat{n}]]dv + \frac{1}{2}\sum_i \int W_0 \sin^2\,\varphi_i\, dS \tag{1}$$

Here the unit vector $\hat{n}$ is the director, the elastic moduli $K_1$, $K_2$, and $K_3$ describe transverse bending (splay), torsion (twist), and longitudinal bending (bend) deformations, respectively, and $K_{24}$ is the surface elastic constant. The last term provides the interaction between the nematic and the confining plates. There, $\varphi_i$ is the angle between $\hat{n}$ and the easy anchoring axis at the plate $i$ ($i=1, 2$), and $W_0$ denotes the strength of interaction in units of energy per area.

We assume that the optical field $\vec{E}$ is strong enough, so that the dielectric tensor of the nematic will depend on the optical field.

The free energy of the nematic also contains an electromagnetic part due to the incident electromagnetic field. As we have already discussed, the first contribution is given by Eq. (1). The electromagnetic free energy, $F_{em}$ is in MKS units,

$$F_{em} = -\frac{1}{2}\mathrm{Re}\left[\int_V \vec{D}\cdot\vec{E}\,dv\right] = -\frac{1}{2}\int_V \left[\varepsilon_{xx}(z)|E_x| + \varepsilon_{zz}(z)|E_z|^2 + \varepsilon_\perp|E_y|^2 + \varepsilon_{xz}(z)\mathrm{Re}(E_xE_z^*)\right]dv \tag{2}$$

where the dielectric tensor $\varepsilon$ has elements:

$$\varepsilon_{ij} = \varepsilon_\perp\delta_{ij} + \varepsilon_a n_i n_j \tag{3}$$

where $\varepsilon_\perp$ and $\varepsilon_\parallel$ are the perpendicular and parallel dielectric constants of the nematic and $\varepsilon_a = \varepsilon_\parallel - \varepsilon_\perp$ is the dielectric anisotropy. The components of the director are

$\hat{\mathbf{n}} = \sin\theta(z)\mathbf{e}_x + \cos\theta(z)\mathbf{e}_z$ where $\mathbf{e}_x$ and $\mathbf{e}_z$ are the unit vectors along the $x$ and $z$ directions, respectively. Since $\hat{\mathbf{n}}$ is a position dependent vector, Eq. (3) shows explicitly that the dielectric tensor is inhomogeneous as well as anisotropic. Using Eqs. (1)–(3), the total free energy, $\mathcal{F}$, becomes

$$\begin{aligned}\mathcal{F} = \mathcal{F}_{el} + \mathcal{F}_{em} = (1/2)\int_V \big[K_1(\nabla\cdot\hat{\mathbf{n}})^2 + K_2(\hat{\mathbf{n}}\cdot\nabla\times\hat{\mathbf{n}})^2 + K_3(\hat{\mathbf{n}}\times\nabla\times\hat{\mathbf{n}})^2 \\ - K_{24}\nabla\cdot[\hat{\mathbf{n}}\nabla\cdot\hat{\mathbf{n}} + \hat{\mathbf{n}}\times\nabla\times\hat{\mathbf{n}}]\big]dv \\ + (1/2)\sum_i \int W_0 \sin^2\,\varphi_i\, dS - (1/2)|E_0|^2\int_V \varepsilon_{xx}(z)dv \end{aligned} \tag{4}$$

which can be transformed in:

$$\begin{aligned}\mathcal{F}/K_1 = \int_0^1 \left(\frac{d\theta}{d\zeta}\right)^2 (\sin^2\,\theta + \eta\cos^2\,\theta)d\zeta + \sigma\sin^2\,\theta(0)/2 \\ + \sigma\sin^2\,\theta(1)/2 - \varepsilon_\perp\int_0^1 |E_x|^2 d\zeta - q\int_0^1 |E_x|^2\sin^2\,\theta d\zeta \end{aligned} \tag{5}$$

where $\eta = K_3/K_1$, $LW_\theta/K_1$, $\zeta = z/L$, $\overline{E}_x = E_x/E_0$, $L$ is the thickness of the slab, and $q$ is a parameter defined as

$$q = \varepsilon_a E_0^2 L^2/K_1 \tag{6}$$

and represents the ratio of the electric to the elastic energies; for $q << 1$ the influence of the applied field is weak, while for $q \gg 1$ the field essentially dominates over the elastic energies. The stationary orientational configuration $\theta(\zeta)$ is determined by minimizing the free energy, Eq. (5). This minimization leads to the Euler-Lagrange Eq. [17] in the bulk

$$0 = \frac{d^2\theta}{d\zeta^2}(\sin^2\,\theta + \eta\cos^2\,\theta) + \frac{1}{2}\left(\frac{d\theta}{d\zeta}\right)^2(1-\eta)\sin 2\theta + \frac{q}{2}|\overline{E}_x|^2\sin 2\theta \tag{7}$$

with the conditions at the plates:

$$\left.\frac{d\theta}{d\zeta}\right|_{\zeta=0} = \left.\frac{\frac{1}{2}\sigma\sin 2\theta}{\sin^2\,\theta + \eta\cos^2\,\theta}\right|_{\zeta=0} \tag{8}$$

$$\left.\frac{d\theta}{d\zeta}\right|_{\zeta=1} = \left.\frac{-\frac{1}{2}\sigma\sin 2\theta}{\sin^2\,\theta + \eta\cos^2\,\theta}\right|_{\zeta=1} \tag{9}$$

The resulting configuration can be obtained by solving Eq. (7) subjected to the conditions given by Eqs. (8) and (9).

## 3. Transverse Magnetic Fields

For simplicity, we are going to consider only the transverse magnetic (TM) field case. The equation governing the propagation of electromagnetic waves through the

nematic are derived from Maxwell's equations without sources which in this case are only $z$ – *depend*. The most general solution for the TM fields can be written in the form

$$\mathcal{H}_y = H_y(\zeta, k_0)\exp[-i\omega t], \tag{10}$$

where $H_y$ is the magnetic field, $\omega$ is the frequency, and $t$ is the time. Inserting Eq. (10) in the wave equation leads to [12]:

$$\frac{dG_x}{d\zeta} + k_0 L H_y = 0 \tag{11}$$

$$G_x = iE_x = \frac{1}{\varepsilon_\perp \varepsilon_{||}} \frac{\varepsilon_{zz}}{k_0 L} \frac{dH_y}{d\zeta} \tag{12}$$

$$E_z = \frac{1}{\varepsilon_\perp \varepsilon_{||}} \frac{i\varepsilon_{zz}}{k_0 L} \frac{dH_y}{d\zeta} \tag{13}$$

## 4. Solutions

Let us consider a plane wave of amplitude $E_0$ that after traveling through an homogeneous isotropic medium impinges normally from the left into the nematic slab (Fig. 1). Then, one part of the wave is reflected back to the homogeneous medium with amplitude $r$. Thus, the electric field in that region can be expressed as

$$\vec{E} = \exp(ik_0 L\zeta)\hat{i} - r\exp(-ik_0 L\zeta)\hat{i}, \quad \zeta < 0 \tag{14}$$

where $\hat{i}$ is the unit vector along $x$. Using Faraday's law, it can be found the corresponding magnetic field

$$\vec{H} = \exp(ik_0 L\zeta)\hat{j} - r\exp(-ik_0 L\zeta)\hat{j}, \quad \zeta < 0 \tag{15}$$

On the other hand, at the right side of the slab a transmitted wave of amplitude $t$ will emerge from the nematic

$$\vec{E} = t\exp(ik_0 L\zeta)\hat{i}, \quad \zeta > 1 \tag{16}$$

whose corresponding magnetic field is

$$\vec{H} = t\exp(ik_0 L\zeta)\hat{j}, \quad \zeta > 1 \tag{17}$$

In order to solve exactly Eq. (11) we shall assume that the nematic slab is surrounded by vacuum and that there is a perpendicularly incident plane wave. In this way the electromagnetic fields should satisfy the boundary conditions:

$$E_x|_{\zeta=0} = 1 - r \tag{18}$$

$$H_y|_{\zeta=0} = 1 + r \tag{19}$$

$$E_x|_{\zeta=1} = t \tag{20}$$

$$H_y|_{\zeta=1} = t \tag{21}$$

Note that, Eqs. (20) and (21) account for the continuity of the tangential magnetic $H_y$ and electric $E_x$ fields at the border of the slab. These condition can be rewritten in the form

$$E_x(1) - H_y(1) = 0 \tag{22}$$

$$H_y(0) = 1 + r, \quad E_x(0) = 1 - r \tag{23}$$

Note that the boundary value problem defined by Eqs. (11)–(13) has two properties: first, it involves coefficients which are real valued functions, and second it is written in terms of self-adjoint differential operators. Thus, its eigenvalues and eigenfunctions are real.

Inserting Eqs. (12) and (13) into Eq. (7) we obtain

$$0 = \frac{d^2\theta}{d\zeta^2}(\sin^2\theta + \eta\cos^2\theta) + \left(\frac{d\theta}{d\zeta}\right)^2(1-\eta)\frac{\sin 2\theta}{2} + q\frac{\sin 2\theta}{2}|E_x|^2$$

We solve this boundary value problem by using the shooting method in which we employ a Runge Kutta algorithm to solve simultaneously Eqs. (10), (11), and (24) by using as initial conditions Eqs. (8) and (23), in order to search the value of $r$ and $\theta(0)$ for which the condition stated in Eqs. (9) and (22) are satisfied. Numerical solutions of Eq. (7) for 5CB at $T_{IN} - T = 10$ with $T_{IN} = 35$, $\eta = 1.316$, $\sigma = 4$, $K_{11} = 1.2 \times 10^{-11}\,N$, $W_\theta/K_{11} = 40\,\mu m^{-1}$ and $K_{24}/K_{11} = 1$ [17] were calculated by using the shooting method [18].

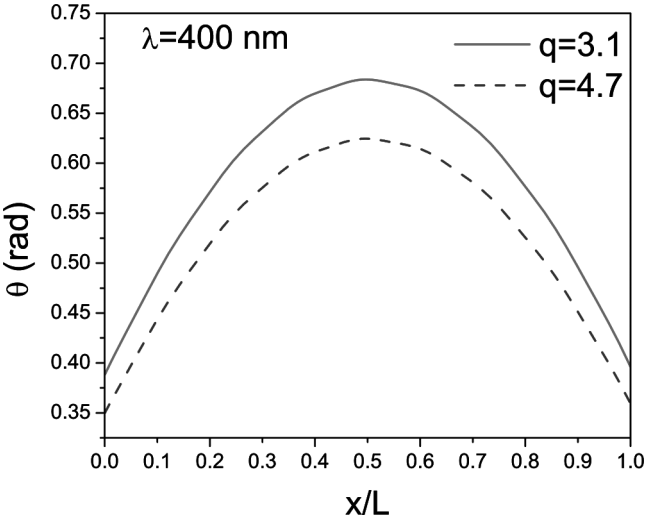


**Figure 2.** Nematic configuration in a planar cell for different intensities (for $\lambda = 400\,nm$).

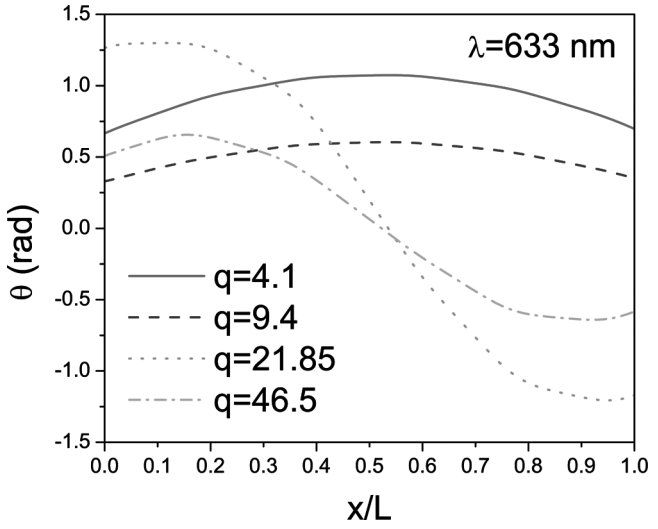


**Figure 3.** Nematic configuration in a planar cell for different intensities for $\lambda = 633$ nm.

## 5. Results

In Figures 2–4 we plot the configuration texture in the cell for different intensities and wavelengths of the electromagnetic wave. Consistently the textures are more distorted as the intensity of the field is increased. Also, as the intensity grows the values of the angle in the plates get far from the easy directions. When the wavelength is larger, from Figures 1 to 3 the configuration is even more distorted. This sequence of plots shows that the nonlinear interaction between the nematic and optical field is stronger when the characteristic length of both systems is nearer.

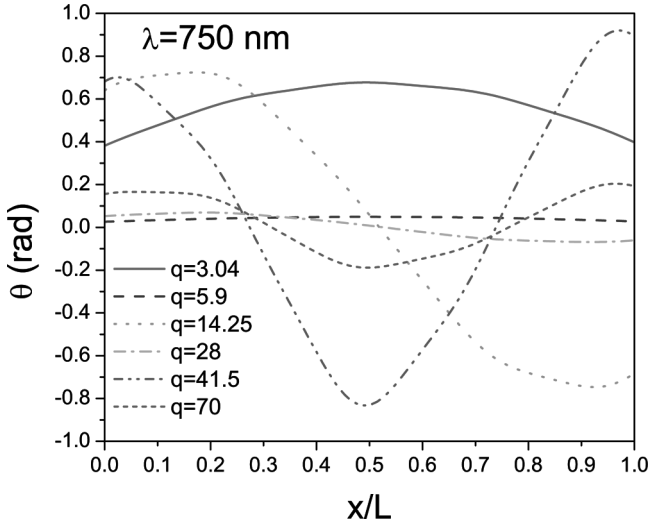


**Figure 4.** Nematic configuration in a planar cell for different intensities for $\lambda = 750$ nm.

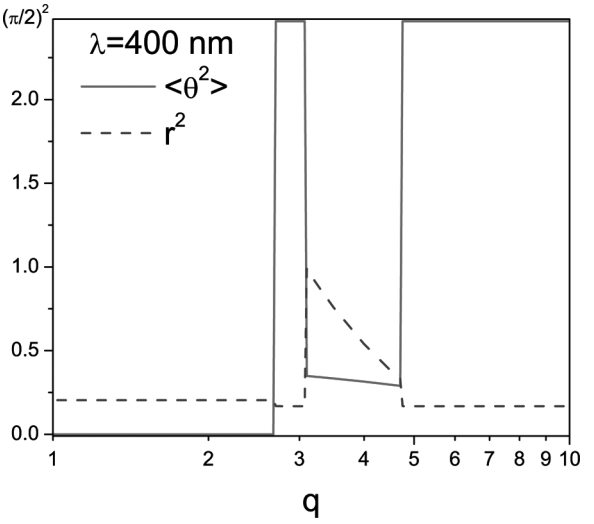


**Figure 5.** Reflectance $r^2$ and average of nematic configuration $\langle\theta^2\rangle$ against intensity field for $\lambda = 400$ nm.

In Figures 5–7 we depict the reflection coefficient $r$ and the average of nematic distortion $\langle\theta^2\rangle$ against the field intensity $q$. All these plots present a band-like structure in the sense that there are intervals of $q$ for which $r$ is very small alternated with regions where $r$ is much larger. The number of these alternating regions augments for larger values of the wavelength as can be seen by comparing Figures 5–7.

In Figures 6 and 7, we can see that the average of nematic orientation $\langle\theta^2\rangle$ also present the same behavior, that is, the distortion is smaller for the same intervals

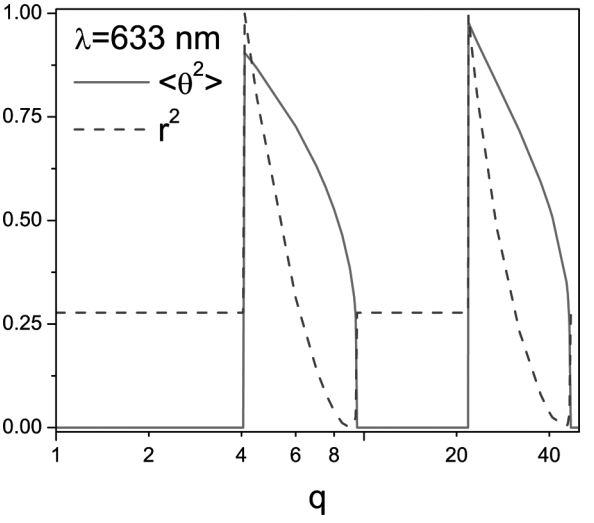


**Figure 6.** Reflectance $r^2$ and average of nematic configuration $\langle\theta^2\rangle$ against intensity field for $\lambda = 633$ nm.

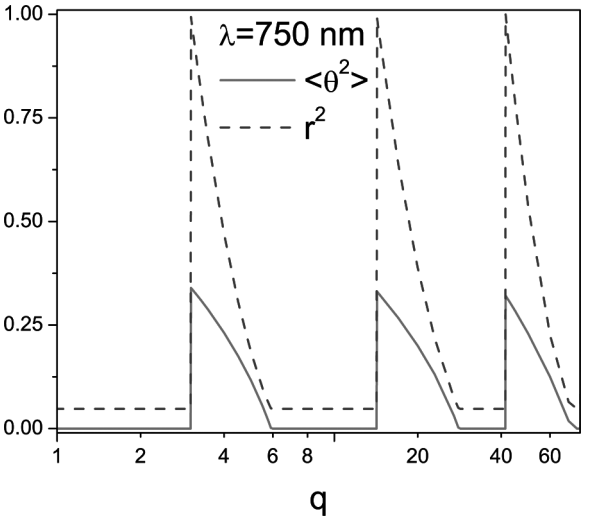


**Figure 7.** Reflectance $r^2$ and average of nematic configuration $\langle\theta^2\rangle$ against intensity field for $\lambda = 750\,\text{nm}$.

of $q$ in which $r$ is small. This implies that the configuration is almost undistorted for those intervals of intensity for which the cell is near transparent for the electromagnetic wave. This is reasonable since an undistorted lossless nematic does not absorb the electromagnetic energy. Notice that Figure 5 corresponds to a wavelength (400 nm) much smaller than the typical length of distortion for this confined liquid crystal (5 μm). This makes the nematic to perceive only the spatial average of the field amplitude and as a consequence the configuration only jumps from zero to $\pi/2$ after a threshold field, except for an interval of $q$ (3.2, 4.8) where the nematic and electromagnetic field couple to give rise to a stop band where the electromagnetic wave is mostly reflected.

## 6. Conclusions

We have considered a nematic liquid crystal confined between two plates in which an electromagnetic field of high intensity impinges normally to the cell and propagates nonlinearly within the nematic. This system is mathematically described by Eqs. (7), (12) and (13) submitted to the boundary conditions expressed by Eqs. (8), (9), (22) and (23).

We have calculated the nematic textures under arbitrary anchoring conditions, versus the position for various field intensities $q$ and wavelengths $\lambda$.

We have obtained a series of stop bands intercalated between transparent regions, as a function of the intensity field for given values of the field wavelength.

## Acknowledgment

We thank partial financial support from project DGAPA-PAPIIT Grant No. IN-115010.

## References


[1] (a) Tabiryan, N. V., Sukhov, A. V., & Zeldovich, B. Ya. (1986). *Mol. Cryst. Liq. Cryst.*, *136*, 1; (b) Khoo, I. C. (1988). *Prog. Optics*, *26*, 108.
[2] Khoo, I. C., & Li, H. (1993). *Appl. Phys. B*, *1*, 573.
[3] Braun, E., Faucheux, L. P., Libchaber, A., McLaughlin, D. W., Muraki, D. J., & Shelley, M. J. (1993). *Europhys Lett.*, *23*, 239.
[4] (a) Conti, C. (2004). *Phys. Rev. Lett.*, *92*, 113902; (b) Conti, C. (2003). *Phys. Rev. Lett.*, *91*, 073901.
[5] Braun, E., Faucheux, L. P., & Libchaber, A. (1993). *Phys. Rev. A*, *48*(1), 611.
[6] McLaughlin, D. W., Muraki, D. J., & Shelley, M. J. (1996). *Physica D*, *97*(4), 471.
[7] Long, X. W., Hu, W., Zhang, T., Guo, Q., Lan, S. S., Gao, X. C. (2007). *Acta Physica Sinica*, *56*, 1397.
[8] Serak, S., & Tabiryan, N. (2006). *Proc. SPIE*, *6332*, 63320Y1–63320Y13.
[9] Karpierz, M. A., Sierakowski, M., & Wolinsky, T. R. (2002). *Mol. Cryst. Liq. Cryst.*, *375*, 313–320.
[10] Izdebskayua, Y., Shvedov, V., Krolikowski, W., Assanto, G., & Kivshar, Y. (2010). *J. Europ. Opt. Soc.*, *5*, 10008.
[11] Abbate, G., De Stefano, L., & Santamato, E. (1996). *J. Opt. Soc. Am. B*, *13*, 1536.
[12] (a) Lin, H., Palffy-Muhoray, P., & Lee, M. A. (1991). *Mol. Cryst. Liq. Cryst.*, *204*, 189; (b) Lin, H., & Palffy-Muhoray, P. (1992). *Optics Lett.*, *17*, 722; (c) Lin, H., & Palffy-Muhoray, P. (1994). *Opt. Lett.*, *19*, 436.
[13] (a) Reyes, J. A., & Rodriguez, R. F. (1997). *Optics Comm.*, *13*, 349; (b) Rodríguez, R. F., & Reyes, J. A. (1999). *Rev. Mex. Fis.*, *45*, 254.
[14] Corella-Madueño, A., Castellanos-Moreno, A., Gutierrez-Lopez, S., & Rosas, R. A., & Reyes, J. A. (2008). *Phys. Rev. E*, *78*, 022701.
[15] Crawford, G. P., Allender, D. W., & Doane, J. W. (1992). *Phys. Rev. A*, *45*, 8693.
[16] Burylov, S. V. (1997). *Zh. Eksp. Teor. Fiz.*, *112*, 1603, [JETP, 85, 873, (1997)].
[17] de Gennes, P. G. (1974). *The Physics of Liquid Crystals*, Clarendon Press: Oxford.
[18] Willian H. Press, *et al*. (1986). *Numerical Recipes: The Art of Scientific Computing*, Cambridge University Press, Cambridge.